

Development of High-Strength and High-Electrical-Conductivity Aluminum Alloys for Power Transmission Conductors

Francisco U. Flores, David N. Seidman, David C. Dunand, and Nhon Q. Vo

Abstract

Using the current processing methods for aluminum conductors, any addition to mechanical strength negatively impacts their electrical conductivity (EC). This trade-off can be seen in common aluminum conductors such as AA1350-H19 which has a relatively high EC ($\sim 61\%$ IACS), but low tensile strength (~ 180 MPa), as opposed to AA6201-T81 having a lower EC ($\sim 52.5\%$ IACS) and higher tensile strength (~ 330 MPa). Presented in this work is the development of new low-cost, scalable 6000-series aluminum conductors with superior combination of mechanical strength and electrical conductivity. By optimizing the thermo-mechanical processing of the aluminum alloy, a synergetic strengthening from precipitation and strain hardening mechanisms is achieved, while the EC loss is minimized. The formation of the strengthening Mg- and Si-rich phase is significantly improved by controlling the Mg and Si concentrations as well as adding inoculant elements to accelerate precipitation kinetics, thus also increasing the alloy's strength. Two alloys stand out in particular: (i) Al-0.7 Mg-0.3Si-0.08Bi aged at 200 °C for 7 h (ultimate tensile strength = 426 MPa and EC = 52.7% IACS); and (ii) Al-0.7 Mg-0.3Si-0.01Sn aged at 200 °C for 4 h (ultimate tensile strength = 445 MPa and EC = 48.2% IACS).

Keywords

Aluminum conductor • High-strength
High-conductivity • Inoculant

Introduction

Due to a better electrical conductivity and lower cost per unit weight compared to copper, pure aluminum and aluminum alloys are the dominant conductors in long-distance power transmission applications, such as high-voltage overhead transmission cables. The most common aluminum wires utilized in high-voltage power transmission applications are the 1000-series, such as AA1350-H19, and the 6000-series, specifically AA6201-T81. The ultimate tensile strength (UTS) of AA1350-H19 is relatively low (~ 180 MPa), while its electrical conductivity (EC) is high (60.9% IACS) [1]. The UTS of AA6201-T81 is higher (~ 330 MPa), while its EC is relatively low (52.5% IACS) [1, 2]. AA6101-T6 is positioned between AA1350-H19 and AA6201-T81, with intermediate values of UTS (~ 220 MPa) and EC (57.7% IACS) [1]. A graph of UTS versus EC for several aluminum alloy series is displayed in Fig. 1. The dotted line in Fig. 1 represents an upper limit for current commercial aluminum alloys in terms of the trade-off between UTS and EC. Attaining values above this line is a challenge since strengthening strategies, such as the addition of alloying elements to form new strengthening phases, typically result in a loss of EC.

Research efforts have been made to develop new aluminum alloy systems that can achieve a combination of tensile strength and electrical conductivity beyond the dotted line in Fig. 1, including alternative processing methods such as high-pressure torsion, a severe plastic deformation process. This was utilized at optimized temperatures to modify refined grain structures and the morphology of the strengthening Mg- and Si-rich phases [1]. The resulting alloys have both high tensile strengths (365–412 MPa) and

F. U. Flores (✉) · D. N. Seidman · N. Q. Vo
NanoAl LLC, Skokie, IL 60077, USA
e-mail: fflores@nanoal.com

D. N. Seidman
e-mail: d-seidman@northwestern.edu

N. Q. Vo
e-mail: nvo@nanoal.com

D. N. Seidman · D. C. Dunand
Materials Science and Engineering, Northwestern University,
Evanston, IL 60208, USA
e-mail: dunand@northwestern.edu

The optimization of the thermo-mechanical processing of AA6201 alloy focused on all steps, namely solutionization, artificial aging and finally cold rolling, to achieve an optimized combination of tensile strength and electrical conductivity. The cast ingots were machined into square rods measuring 2.65 mm in width. The rods were solution heat-treated at 560 °C for 2 h, followed by room temperature aging of about 2 h. Various durations for subsequent artificial aging at 200 °C were studied to identify the peak-aging condition after solutionization. The artificial aging was followed by cold rolling into a square wire with area reduction ratio (A/A_0) of 10. Five EC measurements at room temperature were performed on each wire sample utilizing a Keithley four-point probe. The same strand of wire was then used to perform a tensile test (two wire samples for each condition) utilizing a 50-kN Shimadzu tensile tester, using crosshead displacement to measure strain. Controls were carried out with T6-(cold rolled, solution heat treated, artificially aged) and T8-(solution heat treated, cold rolled, artificially aged) heat-treatments.

Additionally, the effects of various inoculants (Sr, In, Sn, Sb, Pb, and Bi) in the Al wire were studied. The concentrations of the inoculants, shown in Table 1, were chosen based on their maximum solid solubilities in binary phase diagrams with Al, all of which were obtained through the ASM Alloy Phase Diagram Database™. The alloys were processed using the same heat treatments as the base alloy to track the UTS and EC evolution.

Results and Discussion

1. Optimized thermo-mechanical process to achieve high-strength and high-conductivity:

Two established thermo-mechanical processes (T6 and T8) and an optimized process (solutionizing at 560 °C for 2 h, room temperature aging for about 2 h, peak aging at 200 °C and cold rolled) were explored to fabricate 2.65 mm (width) square wires from the base AA6201 alloy (all cold rolled to $A/A_0 = 10$). The aging step—either before cold-working for the optimized process or after cold-working for the T8- and T6-commercial tempers—various temperatures and times were studied to identify the peak-aging condition. The best combination of UTS and EC is defined by the data point that is highest above the dotted diagonal line in Fig. 1, representing the limit of current commercial aluminum alloys in terms of obtaining both UTS and high EC. The optimized thermo-mechanical process, where solutionization and

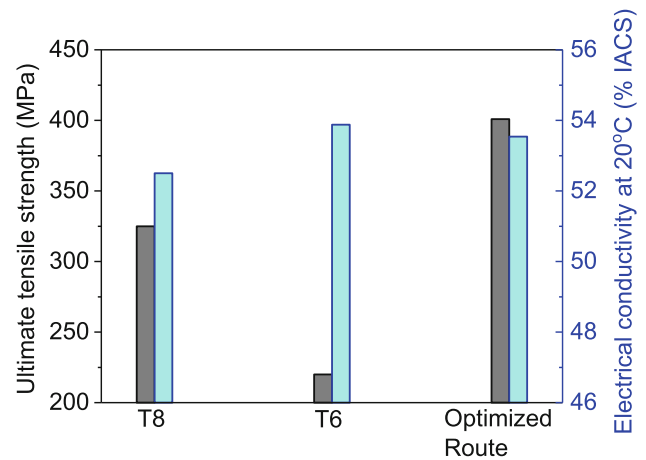


Fig. 2 Ultimate tensile strength and electrical conductivity at 20 °C of 2.65 mm (width) square wires for the base alloy shown in Table 1, each processed by different thermo-mechanical paths (T8-, T6-, and the optimized process)

artificial aging precede cold rolling, yields a superior combination of tensile strength and electrical conductivity. Commercial properties for the T6 and T8 processing route (displayed in introduction) were confirmed in the lab-produced wires for control purposes. The data collected for these processes is shown in Fig. 2.

The different UTS and EC values obtained in the three studied thermo-mechanical paths can be correlated to the microstructures obtained for each process. The T8-temper, with peak-aging occurring after cold-working, results in Mg- and Si-rich strengthening precipitates forming at grain boundaries. In this case, the precipitates are relatively coarse and not effective as strengtheners. Strain hardening from cold-working decreases slightly from the aging step. The T6-temper, with solutionizing and peak-aging occurring after cold working, results in formation of Mg- and Si-rich precipitates, which is the only strengthening mechanism; thus, it yields a relatively low UTS. The T6-temper permits full precipitation of Mg and Si solute atoms, resulting in a higher EC, compared to the T8-temper. Finally, the optimized thermo-mechanical process, with the solutionizing and peak-aging steps occurring before cold-working, results in the formation of Mg- and Si-rich strengthening precipitates, followed by strain-hardening from cold-working. In this case, the wire is hardened by both strengthening mechanisms, which yields a high UTS. This process also yields the highest EC among the three tempers, suggesting that the α -Al matrix contains the lowest residual concentrations of Mg and Si atoms from a complete precipitation of the Mg- and Si-rich phase. In conclusion, it is found that the

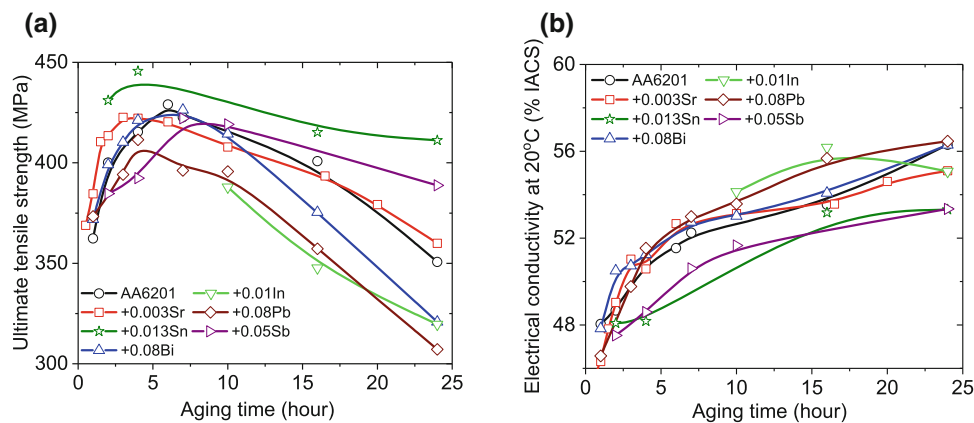


Fig. 3 **a** Ultimate tensile strength and **b** electrical conductivity at 20 °C of the 2.65 mm (width) square wires as a function of peak-aging time at 200 °C, which are comprised of compositions shown in Table 1,

with additions of different inoculant elements. Error bars of a few data points are omitted for figure clarity

optimized process outperforms T6- and T8-temper for wires that have both high strength and electrical conductivity in the 6000-series aluminum alloys.

2. Effects of inoculant elements in Al–Mg–Si-based alloy:

Prior studies demonstrate that the addition of inoculants, Sr [9] and Sn [10, 11], in Al–Mg–Si-based alloys increases the mechanical strength, while maintaining the electrical conductivity, of the base alloys. Thus, a systematic study was done to investigate the effects of Sr and Sn, as well as several other inoculants (In, Sb, Pb, and Bi) in the studied AA6201 wires, processed by the optimized processing route. Figure 3a displays the UTS as a function of peak-aging time from 0 to 24 h at 200 °C. For the base AA6201 alloy, UTS of the wire increases up to ~7 h, then decreasing at longer aging times. This trend corresponds to the precipitation of Mg- and Si-rich precipitates, which peaks at ~7 h of aging. Beyond this aging time, the precipitates are coarsened, thus losing their strengthening effect. Figure 2b displays the EC as a function of aging time from 0 to 24 h at 200 °C. For the base AA6201, EC of the wires rapidly increases up to 7 h, the peak-aging condition for strength, then gradually increases for longer times.

Figure 3a, b shows that inoculant elements have a strong influence on the evolution of UTS and EC during the aging process. Prior studies assign this effect to the modified precipitation kinetics of Al–Mg–Si alloys by addition of

inoculant elements [9–11]. In this study, addition of 0.003% Sr, 0.013% Sn or 0.08% Pb reduce the peak-aging time from 7 to 4 h. Addition of 0.013% Sn is the most effective in increasing the peak-strength, reaching 445 MPa in UTS. Addition of 0.08% Bi, 0.01% In or 0.08% Pb results in a lower strength after aging for 24 h, compared to the base inoculant-free AA6201 alloy, showing that these elements possibly accelerate coarsening kinetics of the strengthening Mg- and Si-rich phase.

To better understand the effect of inoculant elements on the combined properties of UTS and EC, Fig. 4 displays plots of UTS and EC for all studied wires. Interestingly, nearly all wires with different inoculants, generally falls on the same trend line, except AA6201+0.013Sn alloy. This suggests that the main effect of the inoculant elements is modifying the precipitation kinetics of the Mg- and Si-rich phase, either accelerating or decelerating it. Even though the peak-aging time changes, the combined properties of UTS and EC fall on the same trend. Figure 4b is the same plot shown in more details, within the UTS range of 350–450 MPa and EC range of 50–56%IACS. The wires that have optimized combinations of UTS and EC are: (i) Al-0.7 Mg-0.3Si-0.08Bi aged at 200 °C for 7 h (UTS = 426 MPa and EC = 52.7%IACS); and (ii) Al-0.7 Mg-0.3Si-0.01Sn aged at 200 °C for 4 h (UTS = 445 MPa and EC = 48.2%IACS). It is noted that AA6201+0.013Sn wire, aged at 200 °C for 4 h, achieves the highest UTS of 445 MPa even though its EC only reaches 48%IACS. This alloy might be useful for those conductor

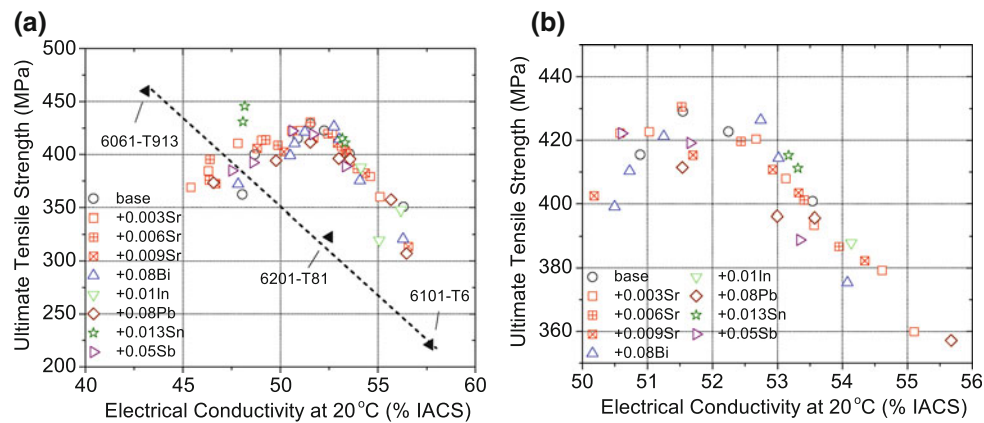


Fig. 4 A map of ultimate tensile strength and electrical conductivity at 20 °C for **a** all investigated 2.65 mm (width) square wires, employing compositions shown in Table 1, with additions of different inoculant

elements and processed by the optimized path. Error bars are omitted for figure clarity; **b** a zoom-in map of **(a)**

applications that focus more on strength than on electrical conductivity.

Conclusions

This work presents a newly developed low-cost, scalable 6000-series aluminum alloys that achieve both high strength and electrical conductivity by: (a) optimizing the thermo-mechanical path to maximize strengthening from precipitation and strain hardening mechanisms, while minimizing loss of electrical conductivity; (b) optimizing the Mg and Si concentrations; (c) adding inoculant elements, which accelerate the precipitation kinetics of the strengthening Mg- and Si-rich phase to increase the alloy's strength; and finally (d) maximizing the area reduction of the cold-working process. This optimized process, in which the solutionizing and peak-aging steps are performed before the alloy is cold-worked to form wires, is the best thermo-mechanical route for fabricating wires that have both high strength and electrical conductivity in the 6000-series aluminum alloys. Moreover, addition of inoculant elements, especially Sn and Bi, further optimizes the combination of ultimate tensile strength and electrical conductivity of the base AA6201 alloy.

Acknowledgements This research was sponsored by Department of Energy—Office of Science under Award Number DE-SC0015232 (Dr. David Forrest, program manager). The authors also gratefully acknowledge General Cable Corporation (Dr. Sriniripurapu, Dr. Sean Culligan) for guidance on material properties of power transmission cables. The authors kindly thank Dr. David Forrest (DOE), Dr. Theresa Miller (DOE), Andrew Halonen (NanoAl), and Joseph Croteau (NanoAl), for useful discussions.

References

1. Valiev RZ, Murashkin MY, Sabirov I (2014) A Nanostructural design to produce high-strength Al alloys with enhanced electrical conductivity. *Scr Mater*, 76, 13–16.
2. Tian L, Anderson I, Riedemann T, Russell TA, Kim H (2013) Prospects for novel deformation processed Al/Ca composite conductors for overhead high voltage direct current (HVDC) power transmission. *Electr Pow Syst Res*, 105, 105.
3. Tian L, Russell A, Anderson I (2014) A dislocation-based, strain-gradient-plasticity strengthening model for deformation processed metal-metal composites. *J Mater Sci*, 49(7), 2787.
4. Russell AM, Anderson IE, Kim HJ, Freichs AE (2014) Aluminum/Alkaline earth metal composites and method for producing same. U.S. patent 8,647,536. 11 February 2014.
5. Thostenson ET, Ren Z, Chou TW (2001) Advances in the science and technology of carbon nanotubes and their composites: A review. *Composites Sci Tech*, 61(13), 1899–1912.
6. Kuzumaki T, Miyazawa K, Ichinose H, Ito K (1998) Processing of carbon nanotube reinforced aluminum composite. *J Mater Res*, 13 (9), 2445–2449.
7. Xu CL, Wei BQ, Ma RZ, Liang J, Ma XK, Wu DH (1999) Fabrication of aluminum-carbon nanotube composites and their electrical properties. *Carbon*, 37(5), 855–858.
8. Noguchi T, Magaria A, Fukazawa S, Shimizu S, Beppu J, Seki M (2004) Carbon nanotube/aluminum composites with uniform dispersion. *Mater Trans*, 45(2), 602–604.
9. Mulazimoglu MH, Zaluska A, Paray F, Gruzleski JE (1997) The effect of strontium on the Mg₂Si precipitation process in 6201 aluminum alloy. *Metall Mater Trans A*, 28(6), 1289.
10. Werinos M, Antrekowitsch H, Kozeschnik E, Eber T, Moszner F, Löffler JF, Uggowitzer PJ, Pogatscher S (2016) Ultrafast artificial aging of Al-Mg-Si alloys. *Scr Mater*, 112, 148–151.
11. Pogatscher S, Antrekowitsch H, Werinos M, Moszner F, Gerstl SSA, Francis MF, Curtin WA, Löffler JF, Uggowitzer PJ (2014) Diffusion on demand to control precipitation aging: Application to Al-Mg-Si Alloy. *PRL*, 112(22), 225701.